Base metal Co-fired (Na,K)NbO$_3$ structures with enhanced piezoelectric performance

Cheng Liu · Peng Liu · Keisuke Kobayashi · Clive A. Randall

Abstract A NaF-Nb$_2$O$_5$ flux doped (Na,K)NbO$_3$ (NKN) based lead-free ceramic was successfully co-fired with nickel inner electrodes in reduced atmospheres. No chemical reactions and/or inter-diffusion were detected at the interface between the nickel (Ni) electrodes and the NKN-based piezoelectrics. Dielectric, resistivity, and electromechanical performance were measured with processing under different firing conditions and flux additions to obtain high densities. Ceramics are obtained with submicron grain structures with the NaF-Nb$_2$O$_5$ sintering aids (2 and 4 wt%) fluxes, and high densities when firing at low pO$_2$ (10^{-10} atms) atmospheres at sintering temperatures ~1150 °C for 2 hours. High resistivities and low losses can be obtained through a second annealing condition at 850 °C and 10^{-7} atms at 8 hours. High d_{33} values (over 350 pm/V) determined under unipolar converse electromechanical measurements were obtained in the simple prototyped co-fired structures to show feasibility towards base metal electrodes in multilayer actuators.

Keywords Lead-free · Piezoelectric · Reduced firing · BME · Cofiring

C. Liu · P. Liu
College of Physics and Information Technology, Shaanxi Normal University, Xi'an, Shaanxi 710062, People's Republic of China

C. Liu · K. Kobayashi · C. A. Randall (✉)
Center for Dielectric Studies, Materials Research Institute, The Pennsylvania State University, University Park, PA 16802, USA
e-mail: car4@psu.edu

K. Kobayashi
Materials R&D Department, R&D Laboratory, Taiyo Yuden Co., Ltd., 5607-2Nakamuroda, Takasaki, Gunma 370-3347, Japan

1 Introduction

Piezoelectric materials have been widely used in actuators, ultrasonic motors, and surface acoustic wave devices due to their excellent electromechanical properties [1–4]. However, most of these materials are lead-based, such as Pb(Zr,Ti)O$_3$ (PZT) and Pb(Mg$_{1/3}$Nb$_{2/3}$)O$_3$-PbTiO$_3$ (PMN-PT), which have raised environmental issues. Although there are a lot of debates on this topic, it is expedient for the piezoelectric community to explore alternative strategies. However, there have been no major breakthroughs beyond the lead perovskites in completely lead free, lead-bismuth perovskite binary and ternary compositions, sometimes referred to as "lead-lite compositions", which have exceeded the performance of the best PZT compositions [5–11]. The highest completely lead-free systems are based on (Na,Bi)TiO$_3$ (NBT) and (Na,K)NbO$_3$ (NKN) [12–17]. NKN-based systems are especially interesting as they have high Curie temperatures (about 420 °C) [14]. However, pure NKN ceramics are difficult to densify in conventional air sintering due to the high volatility of alkaline elements through their sub-oxides at high sintering temperatures, and also a relatively low liquidus-solidus gap in the binary phase diagram [18]. Furthermore, the basic piezoelectric performance of these lead-free piezoelectric candidates is relatively low with direct comparison with the best lead-based piezoelectrics; this is especially the case for actuator based applications [14, 15, 19–21].

Multilayer actuator structures are one solution to engineering higher electromechanical displacements over the lower basic materials performance through decreasing the active layer thickness and increasing the number of electrodes. PZT based multilayered piezoelectric ceramics are commercially produced with co-fired silver-palladium (Ag-Pd) and copper (Cu) inner electrodes [22]. However, with the lower piezoelectric performance and the higher firing condition, the

devices need more electrodes, and so Ag-Pd increases the production costs, and the Cu requires firing at temperatures between 900 and 1020 °C, which is also challenging with the NKN systems that are typically fired above the melting temperature of Cu. So nickel (Ni) inner electrodes are an important alternative base metal electrode system but should be fired in reduced atmospheres.

It is recently reported that an NKN-based system shows a capability of co-firing with Ni inner electrode under low pO_2 atmospheres based on mixtures of nitrogen and hydrogen gases [18, 23]. In our earlier studies, we reported an enhancement of sinterability and piezoelectric performance of NKN-based ceramics via a superior flux—NaF with excess Nb_2O_5 (NaF-Nb_2O_5) [24]. Here we extend this investigation of Ni co-firing with NKN piezoelectric ceramics in low pO_2 atmospheres.

2 Experimental procedures

2.1 Powder preparation

$x(NaF$-$0.5Nb_2O_5)$-$(1$-$x)[Na_{0.5}K_{0.5}(Nb_{0.8}Ta_{0.2})O_3]$ (abbreviated as $100x$NN-NKNT, x=0.02, 0.04, 0.06) powders were synthesized via a solid-state reaction method. The starting materials used in this study were all reagent grade NaF, K_2CO_3, Na_2CO_3, Ta_2O_5, Nb_2O_5 (>99.5 % purity, Alfa Aesar, Ward Hill, MA) and were pre-dried at 200 °C for 24 hours to minimize humidity effects and aid in the weighing out of all stoichiometric ratios. NKNT powders were accurately weighed in stoichiometric ratios and ball milled with zirconia media and ethanol for 24 hours. After the calcination process at 900 °C for 4 hours, different amounts of NaF-Nb_2O_5 flux were later added into NKNT powders and milled for another 24 hours. Then the $100x$NN-NKNT powders were dried and divided into two groups: one group was subsequently granulated and pressed into disk-shaped pellet of 10 mm diameter for density and microstructure characterization; another group of samples was processed via a tape casting method to fabricate co-fired multilayer piezoelectric actuators. The tape casting approach is outlined below.

2.2 Co-fired BME NKN processing

The cofired-actuator structures were prepared via the tape casting method, which has also been adopted in fabricating single dielectric layer capacitors in our laboratory [25]. The calcined powders was first mixed in a solution (named Vehicle A), which consisted of 32 wt% methylethylketone (MEK, Alfa Aesar, Ward Hill, MA), 32 wt% ethyl alcohol (Pharmco—AAPER, Brookfield, CT), and 1 wt% fish oil (Z-3 Blown Menhaden, Tape Casting Warehouse, Yardley, PA) as a dispersant. Then the powder mixed solution was ball milled with zirconia media (9 mm height and 9 mm diameter, TOSOH Ceramics, Tokyo, Japan) for 24 hours. Vehicle B, containing 10 wt% PVB binder (BMS FB–C96, Sekisui, Tokyo, Japan) and 4 wt% plasticizer (Butyl Benzyl Phthalate S-160, Tape Casting Warehouse, Yardley, PA), was added to the solution and followed by an additional 20 hours ball milling. Before tape casting, the slurry was slowly rotated for 6 hours to aid in the removal of air. Tape casting was performed on a sheet of Mylar using a commercial casting machine (A. J. Carstern Co. Inc., Powell River, Canada), with a casting speed of about 8 cm/s. The thickness of the tape was controlled by changing the space between the doctor blade and the casting stage. The resulting tape thickness ranged from about 75 to 80 μm. The tape was dried at least 1 h after casting before the printing and stacking processes. Ni electrode paste was mixed with 55 wt% Ni electrode powder (NI-609 s, Shoei Chemical Inc., Osaka, Japan), 8.5 wt% ceramic powder, 3 wt% ethyl cellulose (Alfa Aesar, Ward Hill, MA), and 33.5 wt% terpineol (Alfa Aesar, Ward Hill, MA). The mixture was grinded and milled for 4 hours and then screen printed on the tape in 2 mm by 3 mm to serve as inner electrodes. Electroded tapes were stacked with a 1 mm offset from each other so that the effective electrode area was approximately 2 mm by 2 mm. More layers were respectively laminated on the top and bottom of the active layer to form cover layers and support the structure (350 μm thick in total for each side). The capacitor structure was stacked together in a uniaxial press at 80 °C for 20 min under 30 MPa, then isostatically laminated (IL-4004, Pacific Trinetics Co., San Marcos, CA) at 80 °C for 20 min under a hydrostatic pressure of 200 MPa. Then these stacked layered sheets with Ni inner electrodes were diced into individual components 6 mm in length and 3 mm in width, followed by a binder burnout at 270 °C for at least 12 hours in air with a heating rate of 0.5 °C/min. The bulk and diced multilayered samples could be sintered within a temperature range of 1100–1200 °C for 2 hours in a reduced atmosphere with pO_2=10^{-10} atm. The furnace was a tube furnace with gas flow controllers that are computer controlled, the pO_2 was monitored with an Oxygen probe sensor (DS probe, Australian Oxytrol Systems, Eaglehawk, Australia) in the furnace. All these as-sintered samples were followed by an annealing process at 850 °C for 8 h in a reduced atmosphere with pO_2=10^{-7} atm. This condition is very similar to the reoxidation conditions used in the fabrication of $BaTiO_3$ based Multilayer Ceramic Capacitor devices, which is selected to minimize the oxygen vacancy concentration, but also selected at conditions that permit no oxidation of the Ni electrodes [26–28]. The terminations to make electrical contact to the inner electrodes are made from the sides. We first polished the sides just sufficiently to expose the inner electrodes for a platinum (Pt) terminal electrodes sputtering. A schematic of the prepared cofired Ni electrode actuator prototype is showed in Fig. 1.
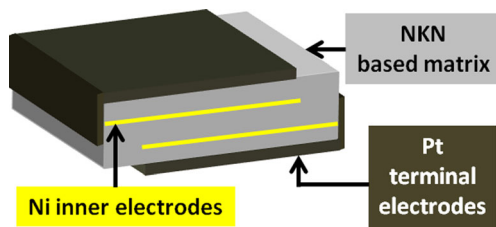
Fig. 1 Schematic of the NKN based ceramic cofired with Ni inner electrodes

2.3 Characterization

The densities of the as-sintered bulk samples were measured by Archimedes method. The relative density was calculated by the expression $\rho_r=\rho_{bulk}/\rho_{theo}\times100$ %, where ρ_r, ρ_{bulk} and ρ_{theo} denoted the relative density, bulk density, and X-ray theoretical density of the samples, respectively. A phase and structure analysis of the as-sintered bulk samples were examined through a X-ray diffractometer (XRD, Philips X'pert Pro MPD, PANalytical Company, Almelo, Holland) with a scanning rate of 10 °/min in the range of 15 °≤2θ≤80 °, using CuKα radiation. Morphology studies of the multilayer cross-section and surface of the actuator prototyped devices were observed using a scanning electron microscope (SEM, S-3500, Hitachi Corp., Tokyo, Japan). Spatial chemical variation through scans across the interfaces was investigated via an energy dispersion spectroscopy (EDS, IMIX X-ray Microanalysis System, Princeton Gamma-Tech, Inc., Princeton, NJ) attached to the SEM. The electrical characterization was extensive. Temperature-dependent dielectric constant and loss tangent were measured by a LCR meter (HP4274A, Agilent Technologies Inc., Santa Clara, CA). The resistivity of the samples was evaluated with a Picoammeter/DC voltage source (HP4140B, Agilent Technologies Inc., Santa Clara, CA) by a two-electrode method at room temperature. Polarization-Electric field (P-E) hysteresis loops and unipolar strain response were measured at 1 Hz with sine waves, using a modified Sawyer-Tower circuit and a linear variable differential strain transducer. High field d_{33} measurements were calculated as the ratio of maximum
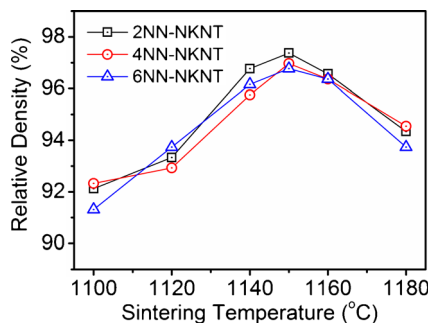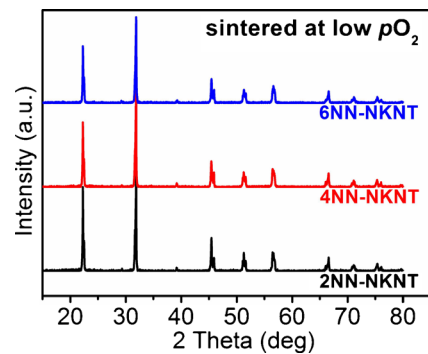

Fig. 3 XRD patterns of the100xNN-NKNT bulk ceramics fired in low pO$_2$ atmospheres

electric-field-induced thickness strain to the maximum electric field.

3 Results and discussion

An important aspect about producing any electroceramic device is to maximize the mechanical strength of the component in the handling and packaging of the system. Typically the maximizing of the densification is important for both mechanical and electrical performance. Figure 2 shows the relative density of the as-sintered 100xNN-NKNT (x=0.02, 0.04, 0.06) ceramics fired within a temperature range of 1100–1180 °C for 2 hours in low pO$_2$ atmospheres, and annealed in a post treatment to improve electrical properties with an annealing process at 850 °C for 8 h in a reduced atmosphere with pO$_2$=10^{-7} atm. The relative densities of the low pO$_2$

Fig. 2 Relative densities of the 100xNN-NKNT bulk ceramics sintered at different temperatures in low pO$_2$ atmospheres
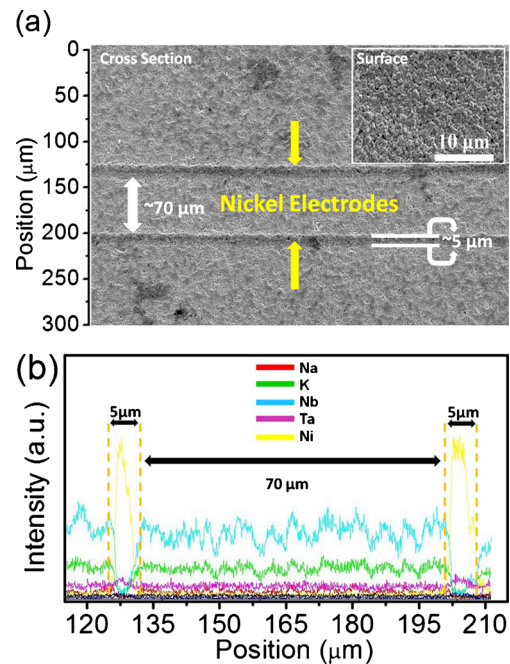
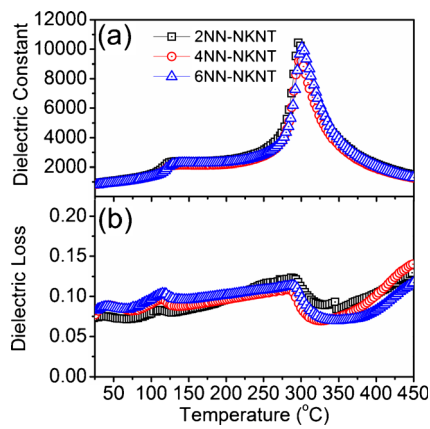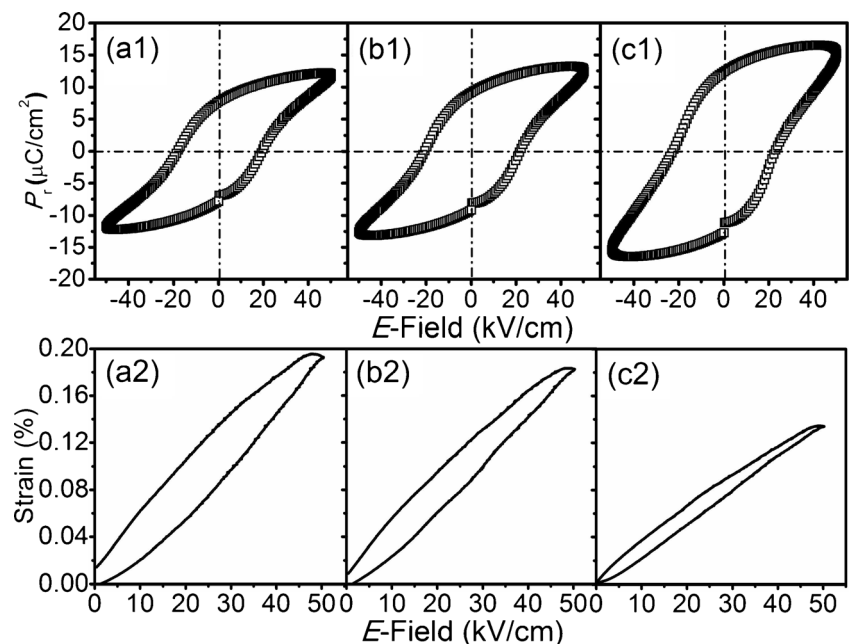Fig. 4 Cross-section SEM morphology(a) and EDS result(b) of the 2NN-NKNT ceramic cofired with Ni inner electrodes

Fig. 5 Temperature dependence of the dielectric properties of the 100xNN-NKNT (x=0.02, 0.04, 0.06) ceramics cofired with Ni inner electrodes

fired bulk samples are increased with the sintering temperatures, reaching up to around 97 % at 1150 °C, and then started to drop through de-densification processes due to extensive grain growth and trapped porosity, and also partial melting. High densities were already obtained in air fired samples using this flux addition [24]. Such densities are typically difficult to achieve in alkaline niobate perovskite ceramics. It should be noted that the optimal sintering temperatures for the low pO_2 fired samples are 50 °C less than those of the air fired specimens [24], consistent with the low pO_2 sintering of the alkali niobates-tantalates lowering the sintering temperatures. For the sake of the cofiring studies, we will only report the sintering temperatures for 1150 °C .

Figure 3 shows room temperature X-ray diffraction (XRD) patterns of the 100xNN-NKNT bulk ceramics sintered at high temperatures 1150 °C for 2 hours in low pO_2 atmospheres. All specimens have diffraction data that could be indexed as orthorhombic symmetry with no detectable secondary phases, indicating that there is no major microstructural difference between the samples fired in air [24] or under reduced atmospheres.

To assess the co-firing, we show in Fig. 4(a) the cross-section SEM micrograph of the co-fired 2NN-NKNT samples. The thicknesses of the ceramic and electrode layer are 70 μm and 5 μm, respectively. The coverage and connectivity of the Ni inner electrode is continuous. The inset of Fig. 4(a) shows the dense surface morphology with highly faceted grains. It is observed that the grain size distribution is homogeneous with an average grain size of~0.8 μm, that is, a fine-grain piezoelectric ceramic relative to typical lead free NKN or PZT microstructures. Furthermore, the EDS data suggest that there is no reaction and/or diffusion between the Ni electrodes and NKN-material, as illustrated in Fig. 4(b).

Figure 5 shows the temperature dependence of the dielectric properties of permittivity and dielectric loss for the 100xNN-NKNT (x=0.02, 0.04, 0.06) Ni co-fired ceramics measured at 10 kHz across a temperature range of 25 to 450 °C. Two displacive phase transitions, the ferroelectric/tetragonal to paraelectric/cubic (T_C) and ferroelectric/orthorhombic to tetragonal (T_{O-T}) phase transitions, as shown in Fig. 5(a), are located around 298 °C and 126 °C, respectively. Compared with the same compositions fired in air [24], the T_C shifts toward higher temperatures (around 8 °C higher) while the T_{O-T} almost stays at the same temperature; as for the dielectric losses, these are also increased slightly with low pO_2 co-firing.

Figure 6 shows the high field electrical and electromechanical properties, the polarization hysteresis (P-E) loops, and

Fig. 6 P-E loops and unipolar S-E curves of the 2NN-NKNT(**a**), 4NN-NKNT(**b**), and 6NN-NKNT (**c**) ceramics cofired with Ni inner electrodes

Table 1 Dc resistivity and dielectric loss values of the 100xNN-NKNT (x=0.02, 0.04, 0.06) ceramics (as-sintered and annealed) cofired with Ni inner electrodes

Samples	ρ ($\Omega\cdot$m) (as-sintered)	ρ ($\Omega\cdot$m) (annealed)	tanδ (as-sintered)	tanδ (annealed)
2NN-NKNT	3.5×10^7	1.6×10^8	0.15	0.073
4NN-NKNT	7.9×10^6	8.3×10^7	0.26	0.077
6NN-NKNT	2.3×10^6	1.8×10^7	0.34	0.081

unipolar strain-electric field (S-E) curves, respectively, for the co-fired 100xNN-NKNT samples measured at room temperature. All specimens exhibit typical ferroelectric hysteresis with well-saturated remnant polarization and no significant space charge. The unipolar S-E curves are exhibited in Fig. 6(a2–c2) below the P-E loops, from which we calculated the high field piezoelectric coefficients via an equation of $d_{33}=S_{max}/E_{max}$ and exhibit the corresponding results in Table 2.

Table 1 compares the dc resistivity and the dielectric loss values of the 100xNN-NKNT (x=0.02, 0.04, 0.06) single-layered ceramics before and after the reoxidation annealing process. It is obvious that the dc resistivity is significantly enhanced and the dielectric loss by an order of magnitude through this heat treatment. After this heat treatment high field bi-polar switching of the ferroelectric and unipolar electromechanical strain field measurements can be performed. Table 2 lists the dielectric and piezoelectric properties of the 100xNN-NKNT (x=0.02, 0.04, 0.06) cofired ceramics (annealed) with Ni inner electrodes. The dielectric properties of the reduced fired monolithic specimens are similar with those of the air-fired samples [24]. However, the E_C values of the reduced fired samples increased about 4 times compared with the air fired specimens; meanwhile, the P_r values decreased with the flux. When $E_{max}=50$ kV/cm, it is noted that the high field d_{33} values for 2NN-NKNT, 4NN-NKNT, and 6NN-NKNT are 385 pm/V, 367 pm/V, and 269 pm/V, respectively.

We anticipate that after processing in low pO_2, the defect concentrations of V_{Na}' and $V_O^{\cdot\cdot}$ are smaller than the air processed case, and the suppressed volatility of the alkali suboxides through rate limited surface diffusion is analogous to our earlier observations of PbO loss in Nb-doped PZT [18, 29]. In addition, the presence of excess NaF can also aid to compensate these vacancies:

$$NaF + 2V_{Na}' + V_o^{\cdot\cdot} \underset{\leftarrow}{\overset{\rightarrow}{}} Na_{Na}^x + F_o^{\cdot} + V_{Na}' \qquad (1)$$
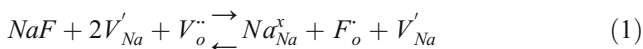
Also, the anionic F$^-$ substitution for the O^{2-} acts as a donor, so the oxygen vacancy concentration is lowered by a number

of scenarios. The domain wall motion would then be expected to be more dynamic and contributes to a higher piezoelectric effect through the extrinsic response.

This paper shows that there is a large potential area of study required in detailed consideration of low pO_2 formulations of NKN piezoelectric ceramics, as it provides an important engineering solution towards multilayer actuator devices with high densities, high electromechanical performance, and low cost with lead free materials. In the exploration for effective sintering fluxes we note that the high field piezoelectric performance can be very sensitive to flux chemistry, for example earlier we used fluxes based on LiF, and here we considered NaF-Nb$_2$O$_5$, and this significantly increased the piezoelectric high field strain, and the microstructure was reduced in size to sub-micron. We wish to point out that although this is an advance in a strategy towards lead free materials, the compositional space across low pO_2 firing conditions and cofiring is largely unexplored in the open literature.

4 Summary and conclusions

NaF-Nb$_2$O$_5$ flux doped NKN-based co-fired piezoelectric ceramics with Ni inner electrodes were successfully fabricated. It was necessary to fire in low pO_2 (10^{-10} atms and 1150 °C for two hours) and then improve the resistivity and dielectric loss with a secondary anneal (850 °C at 10^{-7} atms for 8 hours) before high fields could be applied and enable ferroelectric switching with negligible space charge polarization. After the annealing processes, high field polarization and strain field measurements were applied, and the resistivity and loss improved by an order of magnitude. No detectable reactions or diffusion between Ni electrodes and NKN-based matrix were observed through a cross sectioned SEM and EDS study. The high field converse piezoelectric d_{33} values of over 350 pm/V are gained in the prototyped actuators and are high for untextured NKN samples. It should also be pointed out that in the electrode configurations used, there is still clamping with the capacitive interdigited electrodes, so

Table 2 Dielectric and piezoelectric properties of the 100xNN-NKNT (x=0.02, 0.04, 0.06) ceramics (annealed) cofired with Ni inner electrodes

Samples	T_C (°C)	T_{O-T} (°C)	ε_r	d_{33} (pm/V, @50 kV/cm)	E_C (kV/cm)	P_r (μC/cm^2)
2NN-NKNT	296	125	900	385	20	7.7
4NN-NKNT	298	128	836	367	21	9.2
6NN-NKNT	300	126	780	269	23	12.5

we expect that higher performance could be released with better electrode design.

References

1. K. Uchino, *Piezoelectric actuator/ultrasonic motors* (Kluwer Academic Publisher, Boston, 1996)
2. C.A. Randall, A. Kelnberger, G.Y. Yang, R.E. Eitel, T.R. Shrout, J. Electroceram. **14**, 177 (2005)
3. L.E. Cross, Relaxor ferroelectrics. Ferroelectrics **76**, 241 (1987)
4. G.H. Haertling, J. Am. Ceram. Soc. **82**, 797 (1999)
5. C.A. Randall, R. Eitel, B. Jones, T.R. Shrout, D.I. Woodward, I.M. Reaney, J. Appl. Phys. **95**, 3633 (2004)
6. S.M. Choi, C.J. Stringer, T.R. Shrout, C.A. Randall, J. Appl. Phys. **98**, 034108 (2005)
7. C.A. Randall, R.E. Eitel, T.R. Shrout, D.I. Woodward, I.M. Reaney, J. Appl. Phys. **93**, 9271 (2003)
8. S. Zhang, C.A. Randall, T.R. Shrout, J. Appl. Phys. **95**, 4291 (2004)
9. S. Zhang, R. Xia, C.A. Randall, T.R. Shrout, R. Duan, R.F. Speyer, J. Mater. Res. **20**, 2067 (2005)
10. I. Grinberg, M.R. Suchomel, W. Dmowski, S.E. Mason, H. Wu, P.K. Davies, A.M. Rappe, Phys. Rev. Lett. **98**, 107601 (2007)
11. M.R. Suchomel, P.K. Davies, J. Appl. Phys. **96**, 4405 (2004)
12. T. Takenaka, K. Maruyama, K. Sakata, Jpn. J. Appl. Phys. **30**, 2236 (1991)
13. H. Nagata, T. Takenaka, J. Eur. Ceram. Soc. **21**, 1299 (2001)
14. G. Shirane, R. Newnham, R. Pepinsky, Phys. Rev. **96**, 581 (1954)
15. L. Egerton, D.M. Dillon, J. Am. Ceram. Soc. **42**, 438 (1959)
16. Y. Saito, H. Takao, T. Tani, T. Nonoyama, K. Takatori, T. Honma, T. Nagaya, M. Nakamura, Nature **432**, 84 (2004)
17. M. Matsubara, T. Yamaguchi, W. Sakamoto, K. Kikuta, T. Yogo, S. Hirano, J. Am. Ceram. Soc. **88**, 1190 (2005)
18. K. Kobayashi, Y. Doshida, Y. Mizuno, C.A. Randall, J. Am. Ceram. Soc. **95**, 2928 (2012)
19. T.R. Shrout, S.J. Zhang, J. Electroceram. **19**, 111 (2007)
20. R.E. Jaeger, L. Egerton, J. Am. Ceram. Soc. **45**, 209 (1962)
21. G.H. Haertling, J. Am. Ceram. Soc. **50**, 329 (1967)
22. K. Uchino, Acta Mater. **46**, 3745 (1998)
23. S. Kawada, M. Kimura, Y. Higuchi, H. Takagi, Appl. Phys. Express **2**, 111401 (2009)
24. C. Liu, P. Liu, K. Kobayashi, W. Qu, C.A. Randall, J. Am. Ceram. Soc. (2013). doi:10.1111/jace.12461
25. H. Ogihara, C.A. Randall, S. Trolier-McKinstry, J. Am. Ceram. Soc. **92**, 1719 (2009)
26. C. Chiang, Y. Lee, F. Shiao, W. Lee, D. Hennings, J. Eur. Ceram. Soc. **32**, 865 (2012)
27. H. Saito, H. Chazono, H. Kishi, N. Yamaoka, Jpn. J. Appl. Phys. **30**, 2307 (1991)
28. D. Hennings, J. Eur. Ceram. Soc. **21**, 1637 (2001)
29. N.J. Donnelly, C.A. Randall, J. Appl. Phys. **109**, 104107 (2011)